15   Dynamic Flow Method

**16   Volumetric Chemisorption: Catalyst
       Characterization by Static Methods**

15 Dynamic Flow Method

15.1 NELSON AND EGGERTSEN CONTINUOUS FLOW METHOD

In 1951, Loebenstein and Deitz [1] described an innovative gas adsorption technique that did not require the use of a vacuum. They adsorbed nitrogen out of a mixture of nitrogen and helium that was passed back and forth over the sample between two burettes by raising and lowering attached mercury columns. Equilibrium was established by noting no further change in pressure with additional cycles. The quantity adsorbed was determined by the pressure decrease at constant volume. Successive data points were acquired by adding more nitrogen at the system. The results obtained by Loebenstein and Deitz agreed with vacuum volumetric measurements on a large variety of samples with a wide range of surface areas. They were also able to establish that the quantities of nitrogen adsorbed were independent of the presence of helium.

Nelson and Eggertsen [2], in 1958, extended the Loebenstein and Dietz technique by continuously flowing a mixture of helium and nitrogen through the powder bed. They used a hot wire thermal conductivity detector to sense the change in effluent gas composition during adsorption and desorption, when the sample cell was immersed into and removed from the bath, respectively. Fig. 15.1 illustrates a simplified continuous flow apparatus. Fig. 15.2 is a schematic of the flow path arrangement using a four-filament thermal conductivity bridge.

In Fig. 15.1, a mixture of adsorptive and carrier gas of known concentration is admitted into the apparatus at 'a'. Valve V_1 is used to control the flow rate. The analytical pressure is the partial pressure of the adsorptive component of the mixture. When the system has been purged, the detectors are zeroed by balancing the bridge (see Fig. 15.8). When the sample cell 'b' is immersed in the coolant, adsorption commences and detector D_B senses the decreased nitrogen concentration. Upon completion of adsorption, D_B again detects the same concentration as D_A and the signal returns to zero. When the coolant is removed, desorption occurs as the sample warms and detector D_B senses the increased nitrogen concentration. Upon completion of desorption, the detectors again sense the same concentration and the signal returns to its initial zero value. Wide tubes 'c' act as ballasts to (i) decrease the linear flow velocity of the gas ensuring its return to ambient temperature prior to entering D_B and (ii) to prevent air being drawn over D_B when the cell is cooled and the gas contracts.
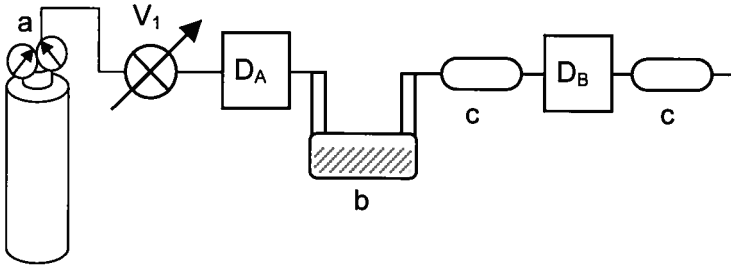
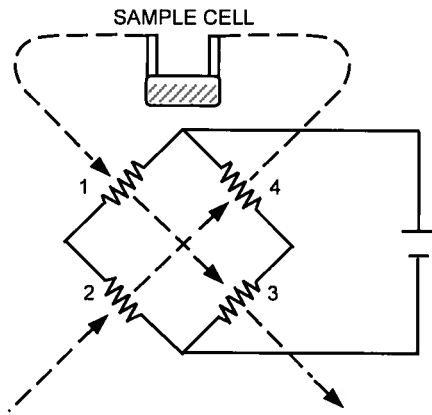*Figure 15.1* Simplified continuous flow apparatus

Figure 15.2 Gas flow path (dashed line) using a four-filament detector. D_A is formed by filaments 2 and 4, $D_B = 1$ and 3. This type of circuit is known as a Wheatstone bridge.
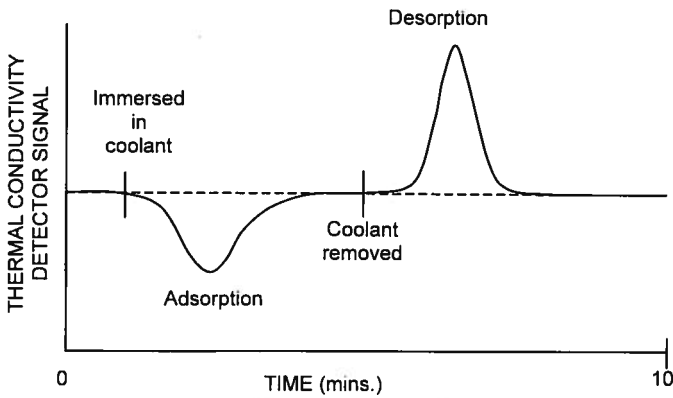
Figure 15.3 Adsorption and desorption peaks in a continuous flow apparatus.

Fig. 15.3 illustrates the detector signals due to adsorption and subsequent desorption. Figs. 15.4 and 15.5 illustrate a parallel flow arrangement which has the advantage of requiring shorter purge times when changing gas composition but is somewhat more wasteful of the mixed gases. The symbols shown in Fig. 15.4 have the same meaning as those used in Fig. 15.1.
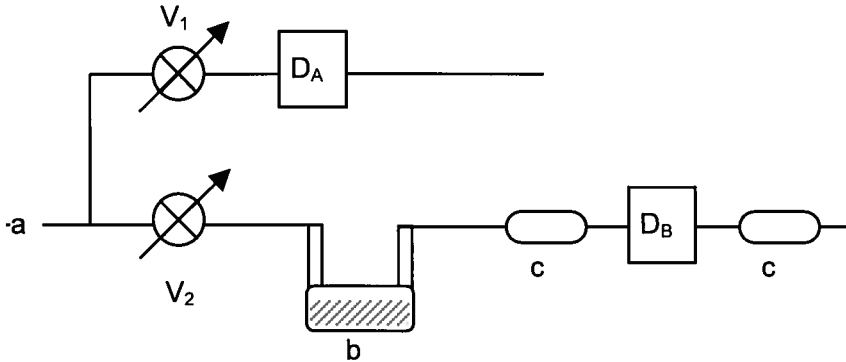
Figure 15.4 Parallel flow circuit.
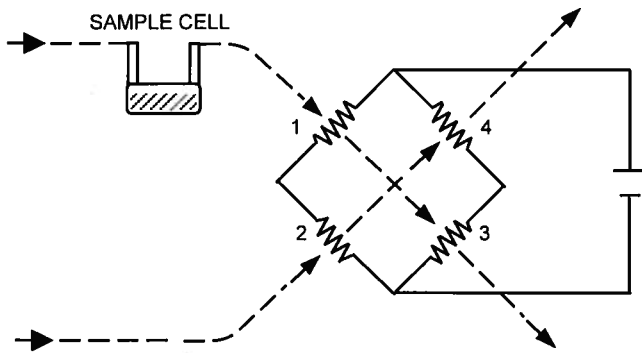
Figure 15.5 Parallel flow path using a four-filament bridge. D_A is formed by filaments 2 and 4 are, 1 and 3 comprise D_B. Dashed lines are gas flow paths.

15.2 CARRIER GAS (HELIUM) AND DETECTOR SENSITIVITY

To be effective, the carrier gas must fulfill two requirements. First, it cannot be adsorbed at the coolant temperature; second, it must possess a thermal conductivity sufficiently different from that of the adsorptive that small concentration changes can be detected. Usually helium is used as a carrier

gas; hence, some discussion regarding the possible influence of helium is necessary.

The forces leading to liquefaction and adsorption are the same in origin and magnitude. Gases substantially above their critical temperature, T_c, cannot be liquefied because their thermal energy is sufficient to overcome their intermolecular potential. Although the adsorption potential of a gas can be greater than the intermolecular potential, helium is, nevertheless, not adsorbed at liquid nitrogen temperature (~77 K) because this temperature is still more than 14 times the critical temperature of helium (~5.3 K).

Furthermore, in order to be considered adsorbed, a molecule must reside on the surface for a time τ at least as long as one vibrational cycle of the adsorbate normal to the surface. The time for one vibration is usually of the order of 10^{-13} seconds which, by equation (15.1), makes τ about 2×10^{-13} seconds at 77 K.

$$\tau = 10^{-13} \exp(100/RT) = 1.91 \times 10^{-13} \sec \qquad (15.1)$$

The value of 100 cal/mol chosen for the adsorption energy of helium is consistent with the fact that helium has no dipole or quadrupole and is only slightly polarizable. Thus, it will minimally interact with any surface. Based upon reflections of a helium beam from LiF and NaCl cleaved surfaces, de Boer [3] estimated the adsorption energy to be less than 100 cal/mol. At 77K the velocity of a helium atom is 638 m/sec, so that in 1.91×10^{13} sec it will travel $1.91 \times 10^{13} \times 638 \times 10^{10} = 1.2$ Å. Thus, the condition that the adsorbate molecules reside near the surface for one vibrational cycle is fulfilled by the normal velocity of helium and not by virtue of its being adsorbed. Stated in alternate terms, the density of helium near a solid surface at 77 K is independent of the surface and is the same as the density remote from the surface. Molecular collisions with the adsorbed film by helium will certainly be no more destructive than collisions made by the adsorbate. In fact, helium collisions will be less disruptive of the adsorbed film structure since the velocity of helium is, on the average, 2.6 times greater than that of nitrogen at the same temperature, while a nitrogen molecule is 7 times heavier. Thus, the momentum exchange due to nitrogen collisions will be the more disruptive. The thermal energy of helium at 77 K is about 220 cal/mol. The heat of vaporization of nitrogen at 77 K is 1.335 kcal/mol, which may be taken as the minimum heat of adsorption. A complete exchange of thermal energy during collisions between a helium atom and an adsorbed nitrogen molecule would not be sufficient to cause desorption of the nitrogen.

To understand the effect of the carrier gas on the response of the thermal conductivity detector, consider the steady state condition that prevails when the resistive heat generated in the hot wire filament is exactly

balanced by the heat conducted away by the gas. This condition is described by equation (15.2)

$$i^2 R = ck(t_f - t_w) \tag{15.2}$$

where i is the filament current, R is the filament resistance, k is the thermal conductivity of the gas mixture, and t_f and t_w are the filament and the wall temperatures, respectively. The constant c is a cell constant that reflects the cell geometry and the separation of the filament from the wall, which acts as the heat sink.

When the gas composition is altered due to adsorption or desorption, the value of k changes by Δk, which in turn alters the filament temperature by Δt_f. Under the new conditions, equation (15.2) can be rewritten as

$$i^2 R = ck(k + \Delta k)(t_f + \Delta t_f - t_w) \tag{15.3}$$

Equating the right hand sight of equations (15.2) and (15.3) gives

$$k(t_f - t_w) = (k + \Delta k)(t_f + \Delta t_f - t_w) \tag{15.4}$$

By neglecting the term $\Delta k \Delta t_f$, a second order effect, equation (15.4) rearranges to

$$\Delta t_f = \frac{\Delta k}{k}(t_w - t_f) \tag{15.5}$$

The change in filament resistance, ΔR, is directly proportional to the small temperature change Δt_f and is given by

$$\Delta R = \alpha R \Delta t_f \tag{15.6}$$

where α is the temperature coefficient of the filament, dependent on its composition, and R is the filament resistance at temperature t_f; thus

$$\Delta R = \alpha R \frac{\Delta k}{k}(t_w - t_f) \tag{15.7}$$

Equation (15.7) requires that Δk be as large as possible for maximum response under a fixed set of operating conditions.

A fortunate set of circumstances leads to a situation in which the same molecular properties that impart minimal interactions or adsorption potentials also lead to the highest thermal conductivities. Molecules of large mass and many degrees of vibrational and rotational freedom tend to be more polarizable and possess dipoles and quadrupoles which give them higher boiling points and stronger interactions with surfaces. These same properties tend to reduce their effectiveness as thermal conductors.

Helium possesses only three degrees of translational freedom and hydrogen the same, plus two rotational and one vibrational degree. However, because of hydrogen's low weight, it has the highest thermal conductivity of all gases, followed by helium. Either of these two gases fulfills the requirement for adequately high thermal conductivities so that Δk in equation (15.7) will be sufficiently large to give good sensitivity with any adsorbate. Helium, however, is usually used in continuous flow analysis because of the hazards associated with hydrogen.

Fig.15.6 is a plot of the thermal conductivity of mixtures of helium and nitrogen obtained on an apparatus similar to that described in the next section. Characteristically, the thermal conductivity of most mixtures does not vary linearly with concentration. The slope of the curve at any point determines the value of Δk and, therefore, the detector response. Fig. 15.6 also illustrates that the greater the difference between thermal conductivities of the adsorbate and carrier gas, the higher will be the slope and therefore the detector response.
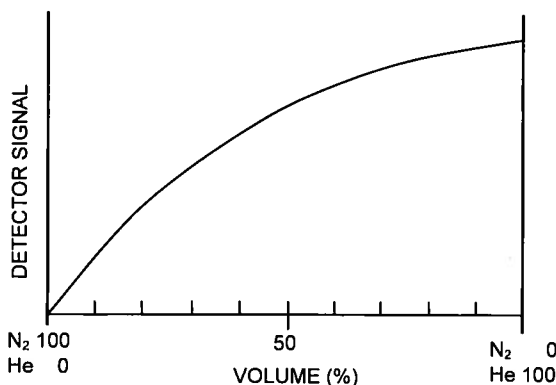

Figure 15.6 Thermal conductivity bridge response.

The shape of the curve shown in Fig. 15.6 is fortuitous in as far as the continuous flow method is concerned. For reasons to be discussed later, the desorption signal (see Fig. 15.3) is generally used to calculate the adsorbed volume. When, for example, 1.0 cm^3 of nitrogen is desorbed into

9.0 cm^3 of helium, the concentration change is 10%. However, when 1.0 cm^3 of nitrogen is desorbed into 9.0 cm^3 of a 90% nitrogen-in-helium mixture, the absolute change is only 1%. Therefore, the increase in slope at high nitrogen concentrations enables smaller concentration changes to be detected when data at high relative pressures are required.

Fig. 15.6 was prepared by flowing helium through one detector while varying the helium to nitrogen concentration ratio through the second detector.

15.3 DESIGN PARAMETERS FOR CONTINUOUS FLOW APPARATUS

The thermal conductivity (T.C.) detector consists of four filaments embedded in a stainless steel or brass block that acts as a heat sink. The T.C. detector is extremely sensitive to temperature changes and should be insulated to prevent temperature excursions during the time in which it takes to complete an adsorption or desorption measurement. Long-term thermal drift is not significant because of the calibration procedure discussed in the next section and, therefore, thermostating is not required. Fig. 15.7 shows a cross-sectional view of a T.C. block and the arrangement of the filaments relative to the flow path. The filaments shown are electrically connected, external to the block, and constitute one of the two detectors.

The filaments must be removed from the flow path, unlike the conventional 'flow over' type used in gas chromatography, because of the extreme flow variations encountered when the sample cell is cooled and subsequently warmed. Flow variations alter the steady state transport from the filaments, leaving them inadequate time to recover before the concentration change from adsorption to desorption is swept into the detector. When this occurs, the baseline from which the signal is measured will be unstable. By removing the filaments from the flow path and allowing diffusion to produce the signal, the problem of perturbing the filaments is completely solved. However, the tradeoff is nonlinear response characteristics. Since the thermal conductivity of the gas mixture is already non-linear with concentration, this additional nonlinearity poses no further problems, and is accommodated by calibration of signals (see §15.4).

A suitable electronic circuit provides power to the filaments and a means of zeroing or balancing the T.C. bridge, adjusting the filament current, attenuating the signal, and adjusting the polarity is shown in Fig. 15.8. Signals produced by adsorption or desorption can be fed to a data acquisition recorder for a continuous trace of the process, and/or to a digital integrator for summing the area under the adsorption and desorption curves.
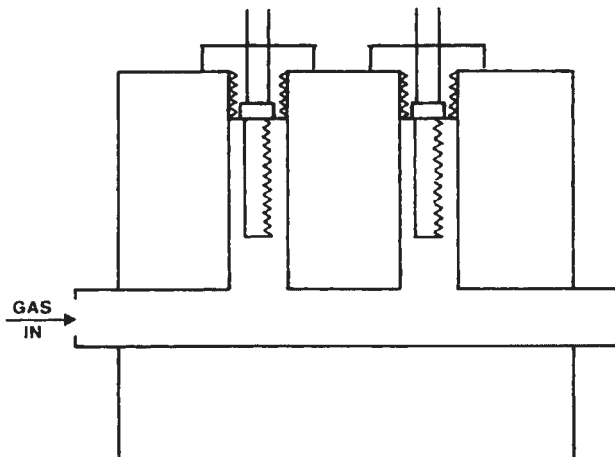
Figure 15.7 Thermal conductivity block with filaments located out of the flow path.
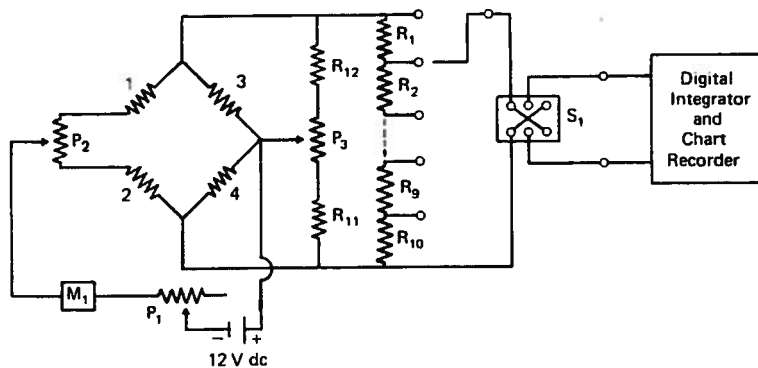

Figure 15.8 Thermal conductivity bridge electronic circuit. 12V dc power supply, stable to 1mV (ripple is not significant due to thermal lag of filaments); P_1, 100 ohms for filament current control; M_1 milliammeter, 0-250 mA; P_2, 2 ohms for coarse zero. Filaments 1 and 4 are detector 1, 2 and 3 are detector 2. P_3, 1 ohm for fine zero; R_{11}, R_{12}, padding resistors ~64ohms; R_1 –R_{10}, attenuation resistors 1, 2, 4, ...512 ohms; S_1 (D.P.D.T.) switch for polarity. Attenuator resistors are ¼ % ww, lowest temperature coefficient; all others are 1%.

Fig. 15.9 is the flow schematic for a commercial continuous flow apparatus. Any one of up to four gas concentrations can be selected from from premixed tanks. Alternatively, adsorptive and carrier can be blended internally by controlling their flows with individual needle valves. A third choice is to feed mixtures to the apparatus from two linear mass flow controllers. Flow meters (operating under pressure to extend their range) indicate input flow rates. A flow meter at the very end of the flow path is

used to calibrate the flow meters. Pressure gauges indicate the input pressure under which the flow meters operate. An optional cold trap removes contaminants from the blended gas stream. After leaving the cold trap, but before flowing into detector D_A, the gas passes through a thermal equilibration tube that reduces the linear flow velocity and thereby provides time for warming back to ambient temperature.

After leaving D_A the flow splits, the larger flow goes to the sample cell at the analysis station, then to a second thermal equilibration tube and a flow meter used to indicate the flow through the sample cell. The smaller flow, controlled by its own needle valve merges with the sample cell effluent before entering detector D_B. The equilibration tubing downstream of D_B serves as a ballast to prevent air from entering D_B when the sample is immersed in the coolant. For high surface areas, the large quantities of desorbed gas can be diverted to a long path (far right). This prevents the gas from reaching the detector before the flow has returned to its original rate.

Splitting the flow as described above serves as a means of diluting the adsorption and desorption peaks in order provide infinitely variable signal height adjustment, in addition to using the stepwise electronic attenuator shown in Fig. 15.8.

A slow flow of adsorptive is directed to the 'out' septum and then to a sample cell positioned at the degas station. The gas flowing through this part of the circuit provides a both source of adsorptive for calibrating detector signals and as a purge for the degas station. Known quantities of adsorptive are injected into the analysis flow through the septum labeled 'in' to simulate a desorption signal for calibration purposes.

To measure the saturated vapor pressure, pure adsorptive is admitted to the P_0 station, when immersed in liquid nitrogen, until it liquefies. The equilibrium pressure is measured on the adjacent transducer.

A diverter valve at the analysis station ensures continuity of flow through the system even when the sample cell is removed.

In order to avoid contamination of the degassed sample when transferring from the degas station to the analysis station, the cells are mounted in spring-loaded self-sealing holders that close when disconnected and open when placed in position.

Sample cells consist of a wide variety of designs for various applications. Fig. 15.10 illustrates seven cells used for various types of samples. Their specific applications and limitations are given in more detail in Section 15.7. Each of the cells shown is made of Pyrex® glass. They are easily filled and cleaned. The cells range from four to five inches in length with stem inside and outside diameters of 0.15 and 0.24 inches, respectively.
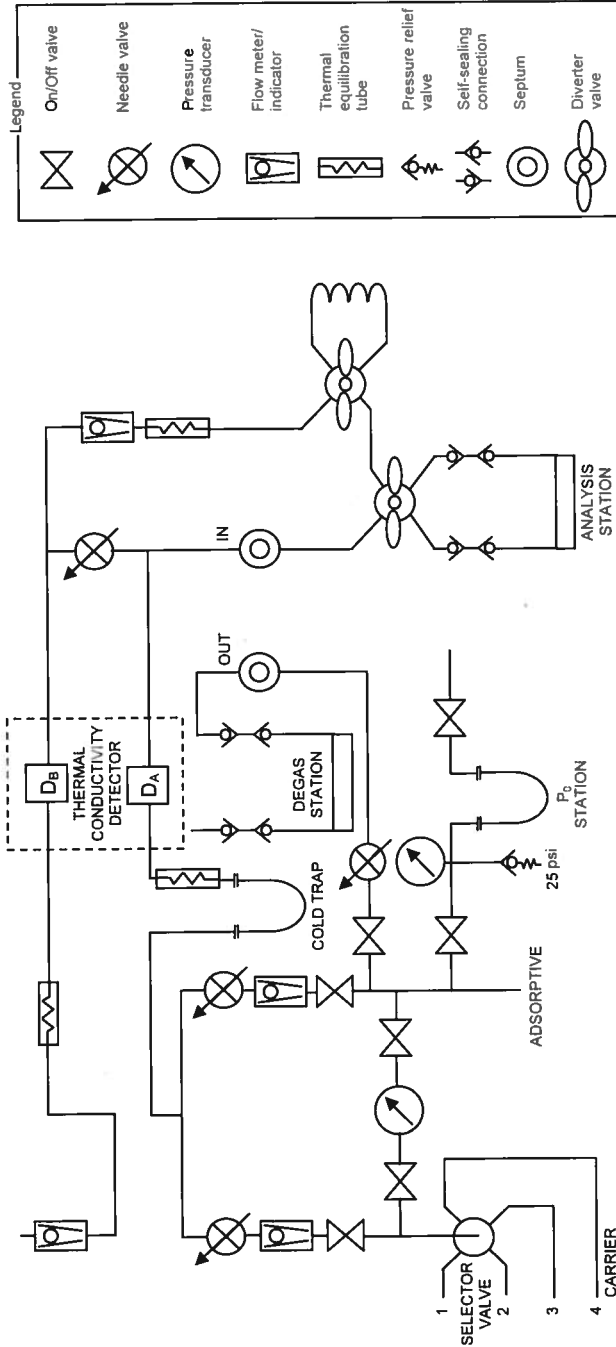
Figure 15.9 Flow diagram for a continuous flow system for adsorption measurements according to the Nelson-Eggertsen method. Not all commercial instruments are equipped with all the features shown.

15.4 SIGNALS AND SIGNAL CALIBRATION

The signal intensity created by an adsorption or desorption peak passing through the detector is dependent upon the attenuator setting, the filament current, and the design of the T.C. detector. Also, as stated previously, the detector response is nonlinear. These circumstances require that the adsorption or desorption signals be calibrated by introducing a volume of carrier or adsorbate gas into the flow stream. An expeditious and accurate method of calibration is the withdrawal of a sample of adsorbate from the 'out' septum (see Fig. 15.9) with a precision gas syringe and the injection of a known volume into the flow stream through the 'in' septum.

    Usually the desorption peak is calibrated because it is free of tailing. By immersing the cell in a beaker of water immediately after removal from the liquid nitrogen, the rate of desorption is hastened. Heat transfer from the water is more rapid than from the air; therefore, a sharp desorption peak is generated. The calibration signal should be within 20% of the desorption signal height in order to reduce detector nonlinearity to a negligible effect.
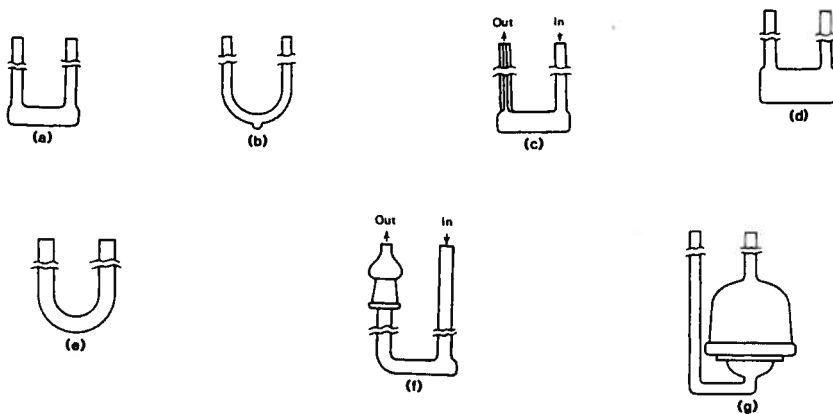

Figure 15.10 Sample cell designs (a) Conventional sample cell — for most powder samples with surface areas greater than 0.2 m^2 in the cell. For samples less than 0.2 m^2, this cell can be used with krypton as the adsorptive. (b) Micro cell —used for very high surface area samples or for low area samples that exhibit thermal diffusion signals. Because of the small capacity of the micro cell, low area samples must be run on high sensitivity settings. (c) Capillary cell — useful for minimizing thermal diffusion signals. Because of the small capacity of the micro cell, low area samples must be run on high sensitivity settings. (d) Macro cell — used with krypton when a large quantity of low area sample is required. Also used for chemisorption when total uptake is small. (e) Large U-tube cell — for larger particles or bulk samples of high area with nitrogen or low area with krypton. (f) Pellet cell — used for pellets or tablets. High surface area with nitrogen or low area samples with krypton. (g) Monolith catalyst cell-for monolithic catalysts and other samples of wide diameter that must be measured as one piece.

The area under the desorption peak, A_d, and the area under the calibration peak, A_c, are used to calculate the volume, V_d, desorbed from the sample according to equation (15.8)

$$V_d = \frac{A_d}{A_c} V_c \qquad\qquad (15.8)$$

where V_c is the volume of adsorptive injected. Equation (15.8) requires no correction for gas nonideality since the volume desorbed is measured at ambient temperature and pressure. Because desorption occurs at room temperature, it is complete and represents exactly the quantity adsorbed. For vapors adsorbed near room temperature, the sample can be heated to ensure complete desorption.
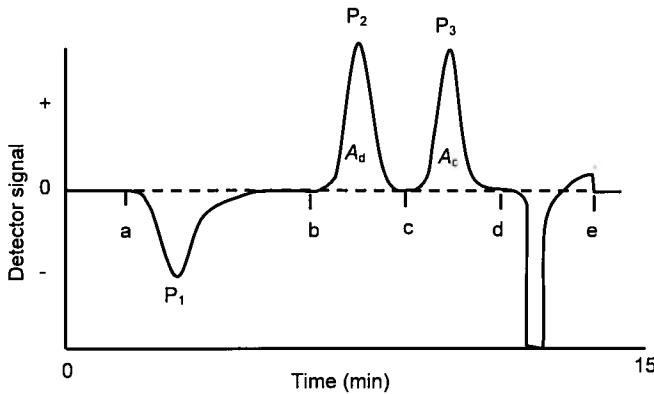

Figure 15.11 Complete cycle for one datum point.

A detailed analysis of the signal record, shown in Fig. 15.11, corresponding to a complete adsorption, desorption, calibration and concentration change cycle discloses that at point a, the sample cell is immersed in the coolant; this action produces the adsorption peak P_1. Point b represents the removal of the coolant bath which leads to the desorption peak P_2. The calibration peak P_3 results from the calibration injection made at point c. At d, a new gas concentration is admitted into the apparatus, which produces a steady base line at e where the detector is re-zeroed and the cycle repeated. The total time for a cycle is usually 15 minutes. Some timesavings can be achieved by combining the purge step (d-e) with the adsorption step (a-b). Familiarity with the apparatus usually allows the operator to choose the correct volume for calibration at particular attenuator and filament current settings or, alternatively, a calibration table can be prepared. If speed is essential, the flow rate can be increased to hasten the

cycle. However, this is at the risk of warming the adsorbent if excessive flow rates are used. Flow rates of 12-15 cm^3/min allow ample time for the gas to equilibrate thermally before reaching the sample powder with all of the cells shown in Fig. 15.10. The presence of helium, with its high thermal conductivity, ensures rapid thermal equilibrium. Therefore, immersion depth of the cell is not critical provided that about 6-7cm (2½ inches) is in the coolant at the flow rates given previously.

Sample cells are not completely filled with powder; room is left above the surface for the unimpeded flow of gas. Although the gas flows over the powder bed and not through it, lower flow rates aid in ensuring against elutriation.

The areas under the adsorption and desorption peaks are usually not exactly the same. This observation is related to the changing slope of Fig. 15.6. Adsorption produces concentration changes to the right, in the direction of decreased sensitivity, while desorption produces signals in the direction of increased sensitivity.

If calibration of the adsorption signal is desired, it is necessary to inject a known quantity of helium. The amount of helium used to calibrate the adsorption signal will usually vary considerably from the amount of nitrogen required for the desorption calibration. This situation arises because, for example, if 1 cm^3 of nitrogen is adsorbed out of a 10% flowing mixture, it will produce the equivalent of 9.0 cm^3 of helium. Therefore, calibration of the adsorption signal will require nine times more helium than the corresponding volume of nitrogen needed to calibrate the desorption signal. If C_{N_2} and C_{He} are the concentrations of nitrogen and helium in the flow stream and if V_{He} is the volume of helium used for calibration, then the volume of nitrogen adsorbed, V_{ads}, is given by

$$V_{ads} = V_{He}\left(\frac{C_{N_2}}{C_{He}}\right)\left(\frac{A_{ads}}{A_{cal}}\right)$$ (15.9)

where A_{ads} and A_{cal} are the areas under the adsorption and calibration signals, respectively.

When small signals are generated, it is difficult to make accurate injections of the required small amounts of gas. Karp and Lowell [4] have offered a solution to this problem that involves the injection of larger volumes of adsorbate diluted with the carrier gas. When a volume containing a mixture of nitrogen and helium, V_{mix}, is injected into the flow stream, the equivalent volume of pure nitrogen, V_{N_2}, is given by

$$V_{N_2} = V_{mix}\left(\frac{X_{N_2} - X'_{N_2}}{X'_{He}}\right) \qquad (15.10)$$

where X_{N_2} is the mole fraction of nitrogen in the calibration mixture and X'_{N_2} and X'_{He} are the mole fractions of nitrogen and helium in the flow stream.

The signals must propagate through the system at identical flow rates. Calibration at a flow rate other than the flow rate associated with the adsorption or desorption peaks can lead to serious errors because the width of the peaks and therefore the peak areas are directly proportional to the flow rate. A good two-stage pressure regulator and needle valve provide adequately constant flow rates over the short time required for desorption and calibration.

Precision gas calibrating syringes can be obtained in various size ranges with no more than 1% volumetric error. Constant stroke adapters provide a high degree of reproducibility. Often, in the BET range of relative pressures, the calibration volumes remain nearly constant because the increased volume adsorbed at higher relative pressures tends to be offset by the decrease in the detector sensitivity. Thus, the same syringe may be used for a wide range of calibrations, which results in the syringe error not effecting the BET slope and only slightly altering the intercept, which usually makes a small contribution to the surface area. A syringe error of 1% will produce an error in surface area far less than 1% for those BET plots with a slope greater than the intercept or for high C values.

15.5 ADSORPTION AND DESORPTION ISOTHERMS BY CONTINUOUS FLOW

To construct the adsorption isotherm, the adsorption, desorption, and calibration cycle shown in Fig. 15.11 is repeated for each datum point required. Errors are not cumulative since each point is independently determined. Relative pressures corresponding to each data point are established by measuring the saturated vapor pressure using any of the preceding methods or by adding 15 torr to ambient pressure. Thus, if X is the mole fraction of adsorbent in the flow stream, the relative pressure is given by

$$\frac{P}{P_0} = \frac{XP_a}{P_a + 15} \qquad (15.11)$$

where P_a is ambient pressure in torr. At the recommended flow rates of 12-15 cm³/min, the flow impedance of the tubing does not raise the pressure in the sample cell.

The method used to construct the adsorption isotherm cannot be used to build the desorption isotherm. This is true because each data point on the adsorption curve reflects the amount adsorbed by a surface initially free of adsorbate. The desorption isotherm, however, must consist of data points indicating the amount desorbed from a surface that was previously saturated with adsorbate and subsequently equilibrated with adsorbate of the desired relative pressure. Karp *et al* [5] demonstrated that the desorption isotherm and hysteresis loop scans can be made in the following manner. First, the sample is exposed, while immersed in the coolant, to a flow of pure adsorbate. The flow is then changed to the desired concentration, leading to some desorption until the surface again equilibrates with the new concentration. The coolant is then removed and the resulting desorption signal is calibrated to give the volume adsorbed on the desorption isotherm. The above procedure is repeated for each datum point required, always starting with a surface first saturated with pure adsorbate.

To scan the hysteresis loop from the adsorption to the desorption isotherm, the sample, immersed in the coolant, is equilibrated with a gas mixture with a relative pressure corresponding to the start of the scan on the desorption isotherm. The adsorbate concentration is then reduced to a value corresponding to a relative pressure between the adsorption and desorption isotherms. When equilibrium is reached, as indicated by a constant detector signal, the coolant is removed and the resulting desorption signal is calibrated. Repetition of this procedure, each time using a slightly different relative pressure between the adsorption and desorption isotherms, yields a hysteresis scan from the adsorption to the desorption isotherm.

To scan from the desorption to the adsorption branch, pure adsorbate is first adsorbed, then the adsorbate concentration is reduced to a value giving a relative pressure corresponding to the start of the scan on the desorption isotherm. When equilibrium is established, as indicated by a constant base line, the adsorbate concentration is increased to give a relative pressure between the desorption and adsorption isotherms. After equilibrium is again established, coolant is removed and the resulting signal is calibrated to yield a data point between the desorption and adsorption isotherms. This procedure repeated, each time using a different final relative pressure, will yield a hysteresis loop scan from the desorption to the adsorption isotherm.

Figs. 15.12 and 15.13 illustrate the results obtained using the above method on a porous amorphous alumina sample. A distinct advantage of the flow system for these measurements is that data points can be obtained where they are desired and not where they happen to occur after dosing, as in the vacuum volumetric method. In addition, desorption isotherms and

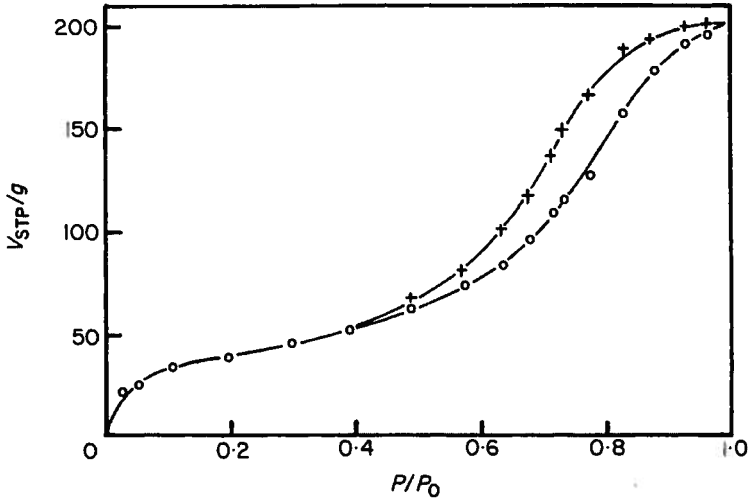hysteresis scans are generated with no error accumulation, void volume measurements, or nonideality corrections.

Figure 15.12 Adsorption and desorption isotherms of N_2 for 0.106 g sample of alumina Adsorption o, Desorption +
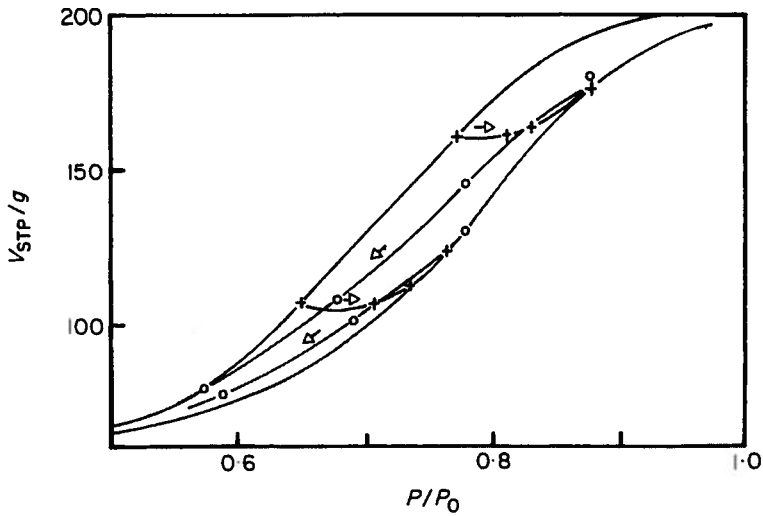

Figure 15.13 Hysteresis loop scan for same sample as Fig. 15.12. Adsorption o, Desorption +

15.6 LOW SURFACE AREA MEASUREMENTS

The thermal conductivity bridge and flow circuits shown in Figs. 15.8 and 15.9 are capable of producing a full-scale signal (1.0 mV) when 0.01 cm^3 of nitrogen are desorbed into a 30% nitrogen and helium mixture. To achieve stable operating conditions at this sensitivity, the thermal conductivity block requires some time to equilibrate thermally and the system must be purged of any contaminants.

A desorbed volume of 0.001 cm^3, using nitrogen as the adsorbate, will correspond to about 0.0028 m^2 (28 cm^2) of surface area if a single adsorbed layer were formed. An equivalent statement is that 0.0028 m^2 is the surface area, measured by the single point method, on a sample which gives a high C value, if 0.001 cm^3 were desorbed. Assuming that a signal 20% of full scale is sufficient to give reasonable accuracy for integration, then the lower limit for surface area measurement using hot wire detection is about 0.0006 m^2 or 6 cm^2. With the use of thermistor detectors, the lower limit would be still smaller.

Long before these extremely small areas can be measured with nitrogen, the phenomenon of thermal diffusion obscures the signals and imposes a higher lower limit [7]. Thermal diffusion results from the tendency of a gas mixture to separate when exposed to a changing temperature gradient. The sample cell is immersed partially into liquid nitrogen. Hence, when the gas mixture enters and leaves the sample cell it encounters a very sharp thermal gradient. This gradient exists along the arm of the tube for *ca*. 2 cm above and below the liquid level, and consequently gases will tend to separate. The extent of separation is proportional to the temperature gradient, the difference in the molecular weights of the two gases and their relative concentrations. The heavier gas tends to settle to the bottom of the cell and as its concentration builds up, a steady state is soon achieved and then the concentration of gas entering and leaving the cell is the same as it was initially. The build up of the heavier gas is only a fraction of a percent and even as low as a few parts per million. Therefore, it does not affect the quantities adsorbed in any measurable way.

However, when the bath is removed and the cell warms up the steady state is disturbed and the slight excess of heavier gas generates a signal followed by a signal due to the excess of lighter gas held up in the "in" arm of the cell. These signals are observed as a negative signal before or after the desorption signal and can generate errors in the integration of the desorption signal. This effect begins to manifest itself with nitrogen and helium mixtures when the total area in the cell is approximately 0.1 - 0.3 m^2

In a static mixture of gases, the amount of thermal diffusion is a function of the time rate of change of the temperature gradient, the gas concentration, and the difference in masses of the molecules. In a flowing

gas mixture, in the presence of adsorption, it is difficult to assess the exact amount of thermal diffusion. Lowell and Karp [8] measured the effect of thermal diffusion on surface areas using the continuous flow method. Fig. 15.14 illustrates a fully developed anomalous desorption signal caused by thermal diffusion. As a result of the positive and negative nature of the signal, accurate integration of the true desorption peak is not possible.
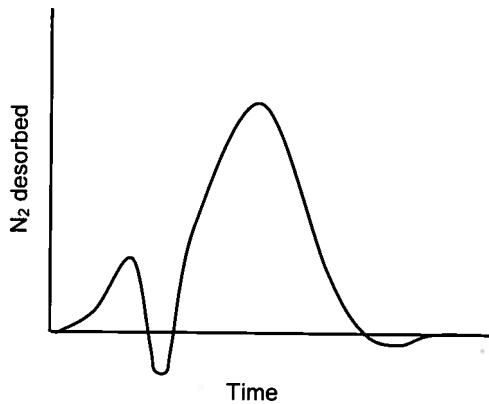

Figure 15.14 Signal shape from desorption of a small volume of nitrogen.

Table 15.1 shows the results of measuring the surface area of various quantities of zinc oxide using a conventional sample cell, Fig. 15.10a. When the same sample was analyzed using a micro cell, Fig. 15.10b, the results obtained were considerably improved, as shown in Table 15.2.

The onset of thermal diffusion depends on the gas concentrations, the sample surface area, the rate at which the sample cools to bath temperature, and the packing efficiency of the powder. In many instances, using a conventional sample cell, surface areas less than 0.1 m^2 can be accurately measured on well-packed samples that exhibit small interparticle void volume. The use of the micro cell (Fig. 15.10b) is predicated on the latter of these observations. Presumably, by decreasing the available volume into which the denser gas can settle, the effects of thermal diffusion can be minimized. Although small sample quantities are used with the micro cell, thermal conductivity detectors are sufficiently sensitive to give ample signal.

Another cell design that aids in minimizing the effects of thermal diffusion is the capillary cell, Fig. 15.10c. By using capillary tubing on the vent side of the cell, a sufficiently high linear flow velocity is maintained to prevent that arm from contributing to the problem. The large sample capacity of the capillary cell, compared to the micro cell, produces sufficient desorption signal to often make the thermal diffusion effect negligibly small.

Table 15.1 Data obtained using conventional cell (measured using the single-point BET method with 20% N$_2$ in He).

Weight	Actual area (m^2)	Measured area (m^2)	Deviation (%)	Signal shape at start of desorption peak
1.305	5.07	5.07	0	
0.739	2.87	2.87	0	
0.378	1.47	1.45	1.4	
0.177	0.678	0.686	−1.2	
0.089	0.345	0.327	5.2	
0.049	0.190	0.166	12.6	
0.0190	0.0730	0.0481	34.1	
0.0101	0.0394	0.0192	51.3	

Lowell [9] published a method to circumvent the problem of thermal diffusion by using an adsorbate with a low vapor pressure, such as krypton, at liquid nitrogen temperature. The coefficient of thermal diffusion $D(t)$ is given by [10]

$$D(t) = \frac{N_1/N_{tot} - N_1'/N_{tot}}{\ln T_1/T_2} \qquad (15.12)$$

where N_1 and N_1' are the adsorbate concentrations at the absolute temperatures T_2 and T_1, respectively with $T_2 > T_1$. The term N_{tot} is the total molecular concentration of adsorbate and carrier gas. Because of krypton's low vapor pressure, its mole fraction in the BET range of relative pressures is of the order of 10^{-4}. This small value causes the difference between N_1/N_{tot} and N_1'/N_{tot} nearly to vanish, with the consequence that no obscuring thermal diffusion signals are generated.

Attempts to increase the size of nitrogen adsorption or desorption signals, by using larger sample cells, results in enhanced thermal diffusion signals due to the increased void volume into which the helium can settle. However, when krypton is used, no thermal diffusion effect is detectable in any of the sample cells shown in Fig. 15.10.

Table 15.2 Data obtained using U-tube cell.

Weight ZnO (g)	Actual Area (m^2)	Measured Area (m^2)*
0.0590	0.2280	0.2300
0.0270	0.1050	0.1020
0.0045	0.0175	0.0161

*This value is corrected by 15 cm^2 for the cell wall area, as estimated from the cell dimensions. Desorption peaks from an empty U-tube cell gave areas of 12- 17 cm^2.

The adsorption signals using krypton-helium mixtures are broad and shallow because the adsorption rate is limited by the low vapor pressure of krypton. The desorption signals are sharp and comparable to those obtained with nitrogen, since the rate of desorption is governed by the rate of heat transfer into the powder bed.

With krypton, the ability to use larger samples of low area powders facilitates measuring low surface areas because larger signals are generated in the absence of thermal diffusion. Also, as is true for nitrogen, krypton measurements do not require void volume evaluations or nonideality corrections, nor is thermal transpiration a factor as in the volumetric measurements.

15.7 DATA REDUCTION—CONTINUOUS FLOW

Table 15.3 can be used as a work sheet for calculating specific surface areas from continuous flow data. The data in the lower left corner are entered first and are used to calculate the other entries. In the example shown, nitrogen is the adsorbate.

Column 1 is the mole fraction of adsorbate in the flow stream. Column 2 is obtained as the product of P_a and column 1. Column 2, when divided by column 3, gives the relative pressure, which is entered in column 4 and from which columns 5 and 6 are calculated. Column 7 is the volume required to calibrate the desorption signal and column 8 is the corresponding weight of the calibration injection, calculated from the equation in the lower left side of the work sheet. The terms A_s and A_c are the areas under the signal and calibration peaks, respectively. Columns 11-13 are calculated from the

data in the previous columns. The data in column 13 are then plotted versus the corresponding relative pressures in column 5. The slope s and intercept i are calculated and the value of W_m is found as the reciprocal of their sum. Equation (4.13) is used to obtain the total sample surface area, S_t, and dividing by the sample weight yields the specific surface area, S.

15.8 SINGLE POINT METHOD

The assumption of a zero intercept reduces the BET equation to equation (5.3). This assumption is, of course, not realizable since it would require a BET C constant of infinity. Nevertheless, many samples possess sufficiently high C values to make the error associated with the single-point method acceptably small (see Chapter 5 and Table 5.2).

Using the zero intercept assumption, the BET equation can be written as

$$W_m = W\left(1 - \frac{P}{P_0}\right)$$

(cf. 5.11)

from which the total surface area can be calculated by

$$S_t = W\left(1 - \frac{P}{P_0}\right)\frac{\overline{N}}{\overline{M}}A_x$$

(cf. 5.12)

From the ideal gas equation of state

$$W = \frac{P_a V \overline{M}}{RT}$$

(15.13)

so that

$$S_t = \left(1 - \frac{P}{P_0}\right)\frac{P_a V \overline{N}}{RT}A_x$$

(15.14)

where P_a and T are the ambient pressure and absolute temperature, respectively, $\overline{N}$ is Avogadro's number, A_x is the adsorbate cross-sectional area, and V is the volume adsorbed.

Table 15.3 Multipoint BET surface area data sheet.

Date: _____ Sample: Titania Total Weight: _____ 12.0434g

Operator: _____ Outgas Procedure: He purge, 1 hr., 150°C Tare: _____ 11.3430g

Sample Weight: 0.7004g

1	2	3	4	5	6	7	8	9	10	11	12	13
X_{N_2}	P (torr)	P_0 (torr)	P/P_0	P_0/P	$(P_0/P)-1$	V_c (cm³)	W_c (g)	A_s	A_c	$W = \dfrac{A_s\,W_c}{A_c}$	$W[(P_0/P)-1]$	$\dfrac{1}{W[(P_0/P)-1]}$
0.050	37.68	768.6	0.0490	20.398	19.398	2.00	0.00230	1066	1083	0.00226	0.0438	22.81
0.100	75.36	768.6	0.0980	10.199	9.199	2.20	0.00252	1078	1050	0.00259	0.0238	41.97
0.200	150.7	768.6	0.1961	5.096	4.096	2.50	0.00287	1168	1098	0.00305	0.0125	80.05
0.2995	225.7	768.6	0.2937	3.405	2.405	2.60	0.00298	1031	879	0.00350	0.0084	118.80

Ambient pressure, $P_a = 753.6$ mm Hg

Vapor pressure, $P_0 = 768.6$ mm Hg

Ambient temperature, T = 295 K

Adsorbate molecular weight, $\overline{M} = 28.01$

Adsorbate area, $A_x = 16.2 \times 10^{-20}$ m²

Calibration gas weight, $W_c = \dfrac{P_a\,\overline{M}\,V_c}{(6.235\times10^4)\,T}$

Plot $\dfrac{1}{W[(P_0/P)-1]}$ vs. P/P_0

Slope, $s = 391.9$

Intercept, $i = 3.52$

$W_m = \dfrac{1}{s+i}$

$W_m = 0.00253$ g

Total surface area,

$$S_t = \frac{W_m\,(6.023\times10^{23})\,A_x}{\overline{M}}$$

$S_t = 8.81$ m²

$S = S_t/W$

$S = 12.58$ m²/g

Using nitrogen as the adsorptive at a concentration of 0.3 mole fraction and assuming P_0 is 15 torr above ambient pressure, equation (15.14) can be expressed as

$$S_t = W\left(1 - \frac{0.3P_a}{P_a + 15}\right)\frac{P_a V \overline{N}}{RT} A_x \tag{15.15}$$

Assuming the ambient pressure P_a is 760 Torr and ambient temperature T is 295 K, equation (15.15) reduces to

$$S_t = 2.84V \,(m^2) \tag{15.16}$$

Thus, the total surface area contained in the sample cell is given by the simple linear relationship above when V is in cubic centimeters. By calibrating the desorption signal, A_{des}, with a known volume of nitrogen, V_{cal}, equation (15.16) can be rewritten as

$$S_t = 2.84\frac{A_{des}}{A_{cal}}V_{cal} \tag{15.17}$$

where A_{des} and A_{cal} are the integrated areas under the desorption and calibration signals, respectively.

Modern commercial single point instruments contain a linearization network that corrects for the hot wire nonlinearity. This procedure allows a built-in digital integrator to integrate the signals linearly so that the surface area is given directly on a digital display. An advantage is that the analysis time for a BET surface area determination is extremely short, usually less than ten minutes [10].

15.9 REFERENCES

1. Loebenstein W.V. and Deitz V.R. (1951) *J. Res. Nat. Bur. Stand.* **46**, 51.
2. Nelson F.M. and Eggertsen F.T. (1958) *Anal. Chem.* **30**, 1387.
3. de Boer J.H. (1953) *The Dynamical Character of Adsorption*, Oxford University Press, London, p33.
4. Karp S. and Lowell S. (1971) *Anal. Chem.* **43**, 1910.
5. Karp S., Lowell S. and Mustaccuiolo A. (1972) *Anal. Chem.* **44**, 2395.
6. Kourilova D. and Krevel M. (1972) *J. Chromat.* **65**, 71.
7. Lowell S. and Karp S. (1972) *Anal. Chem.* **44**, 1706.
8. Lowell S. (1973) *Anal. Chem.* **45**, 8.
9. Benson S.W. (1960) *The Foundation of Chemical Kinetics*, McGraw-Hill, New York, p188.
10. Quantachrome Instruments, Boynton Beach, FL.

Characterization of Porous Solids and Powders: Surface Area, Pore Size and Density

by

S. LOWELL

Quantachrome Instruments, Boynton Beach, U.S.A.

JOAN E. SHIELDS

C.W. Post Campus of Long Island University, U.S.A.

MARTIN A. THOMAS

Quantachrome Instruments, Boynton Beach, U.S.A.

and

MATTHIAS THOMMES

Quantachrome Instruments, Boynton Beach, U.S.A.

Printed on acid-free paper